DOI: 10.1002/adfm.200700436

Nanodot-Enhanced High-Efficiency Pure-White Organic Light-Emitting Diodes with Mixed-Host Structures**

By *Jwo-Huei Jou*,* *Cheng-Chung Chen*, *Yu-Chiao Chung*, *Mao-Feng Hsu*, *Ching-Hsuan Wu*, *Shih-Ming Shen*, *Ming-Hsuan Wu*, *Wei-Ben Wang*, *Yung-Cheng Tsai*, *Chung-Pei Wang*, and *Jing-Jong Shyue*

A relatively high-efficiency, fluorescent pure-white organic light-emitting diode was fabricated using a polysilicic acid (PSA) nanodot-embedded polymeric hole-transporting layer (HTL). The diode employed a mixed host in the single emissive layer, which comprised 0.5 wt % yellow 5,6,11,12-tetra-phenylnaphthacene doped in the mixed host of 50 % 2-(*N*,*N*-diphenyl-amino)-6-[4-(*N*,*N*-diphenylamino)styryl]naphthalene and 50 % *N*,*N*′-bis-(1-naphthyl)-*N*,*N*′-diphenyl-1,10-biphenyl-4-4′-diamine. By incorporating 7 wt % 3 nm PSA nanodot into the HTL of poly(3,4-ethylene-dioxythiophene)-poly-(styrenesulfonate), the efficiency at 100 cd m^{-2} was increased from 13.5 lm W^{-1} (14.7 cd A^{-1}; EQE: 7.2 %) to 17.1 lm W^{-1} (17.6 cd A^{-1}; EQE: 8.3 %). The marked efficiency improvement may be attributed to the introduction of the PSA nanodot, leading to a better carrier-injection-balance.

1. Introduction

White organic light-emitting diodes (OLEDs) have highly promising applications as full-color flat-panel displays, for liquid-crystal-display backlighting and for area illumination.[1–4] The power or current efficiency of white OLEDs is currently one of the primary research concerns. The emissive layer of such a device can be made of phosphorescent and/or fluorescent materials.[3,5–15] For a white OLED with a mixed phosphorescent and fluorescent system, the best power efficiency at 100 cd m^{-2} or above is 37 lm W^{-1}, as reported by Forrest's group.[16] For phosphorescent white OLEDs, Kido's group reported a power efficiency of 36 lm W^{-1}, or 57 lm W^{-1} with an antireflection coating.[9] For polymer-based fluorescent white OLEDs, Yang's group reported a value of 14 lm W^{-1} and So's OSRAM group found an efficiency of 16 lm W^{-1}. For molecular-based fluorescent pure-white OLEDs, the best-reported power efficiency is 6.8 lm W^{-1},[10] which is comparatively low.

The low efficiency of fluorescent white OLEDs may be mainly attributed to their intrinsically low internal quantum efficiency. Besides developing more efficient electro-fluorescent host and guest materials, some architectural approaches have been found to be effective in fabricating high-efficiency fluorescent and phosphorescent white OLEDs.[11,17] The approaches that have been used are to reduce the barriers to carrier injection, balance the carrier injection, confine the entering carriers and the generated excitons in the emissive zone, and facilitate the energy transfer from host to guest. Moreover, the incorporation of nanodots has also been found to be effective in improving the efficiency.[18,19] Nanodots may be incorporated using a dry process. However, poor size or dispersion control may often result. To solve this problem, a wet process must be used. One advantage of a wet process is its feasibility for large areas and roll-to-roll fabrication.[20] In order to achieve a high power efficiency, the OLED device must be relatively thin, which greatly limits the use of large nanodots, especially those with a size comparable to or even greater than the thickness of the layer(s) in which they are to be incorporated.

In this report, we demonstrate the incorporation of small polysilicic acid (PSA) nanodots in a thin hole-transporting layer (HTL) of poly(3,4-ethylene- dioxythiophene)-poly-(styrenesulfonate) (PEDOT:PSS) to enhance markedly the efficiency of a fluorescent pure-white OLED. The device consisted of a 1,250-Å indium tin oxide (ITO) layer, a 300-Å PEDOT:PSS HTL incorporating 7.0 wt % PSA nanodots, a 300-Å white emissive layer, a 400-Å 1,3,5-tris(*N*-phenyl benzimidazol-2-yl)benzene (TPBi) electron-transporting layer, a 10-Å lithium fluoride layer and a 1,500-Å aluminum layer. The incorporated PSA nanodots were prepared by hydrolysis and condensation of sodium metasilicate in 2.5 N hydrochloric acid solution for 40 minutes. They had an average size of 3 nm as determined by dynamic light scattering (see Fig. 1).[21] The white emissive layer was made up of a mixed-host of 50 wt % 2-(*N*,*N*-diphenyl-amino)-6-[4-(*N*,*N*-diphenylamino)styryl] naphthalene (DPASN) and a 50 wt % *N*,*N*′-bis-(1-naphthyl)-*N*,*N*′-diphenyl-1,10-biphenyl-4-4′-diamine (NPB), doped with 0.5 wt % yellow-light-emitting 5,6,11,12-tetra-phenylnaphthacene (Rubrene). The

[*] Prof. J.-H. Jou, C.-C. Chen, Y.-C. Chung, M.-F. Hsu, C.-H. Wu, S.-M. Shen, M.-H. Wu, W.-B. Wang, Y.-C. Tsai, Dr. C.-P. Wang, Dr. J.-J. Shyue[+]
Department of Materials Science and Engineering
National Tsing Hua University
Hsin-Chu 30013 (Taiwan Republic of China)
E-mail: jjou@mx.nthu.edu.tw

[+] Present address: Research Center for Applied Sciences Academia Sinica, 128 Academia Rd., Sec. 2 Nankang, Taipei 11529, Taiwan Republic of China.

[**] The authors would like to thank Prof. F. S. Juang of Institute of Electro-Optical and Materials Science, National Formosa University, for help with the external quantum efficiency and lifetime measurements. This work was financially supported under NSC95-2221-E-007-128-MY3 and AFOSR-AOARD-05-0488.

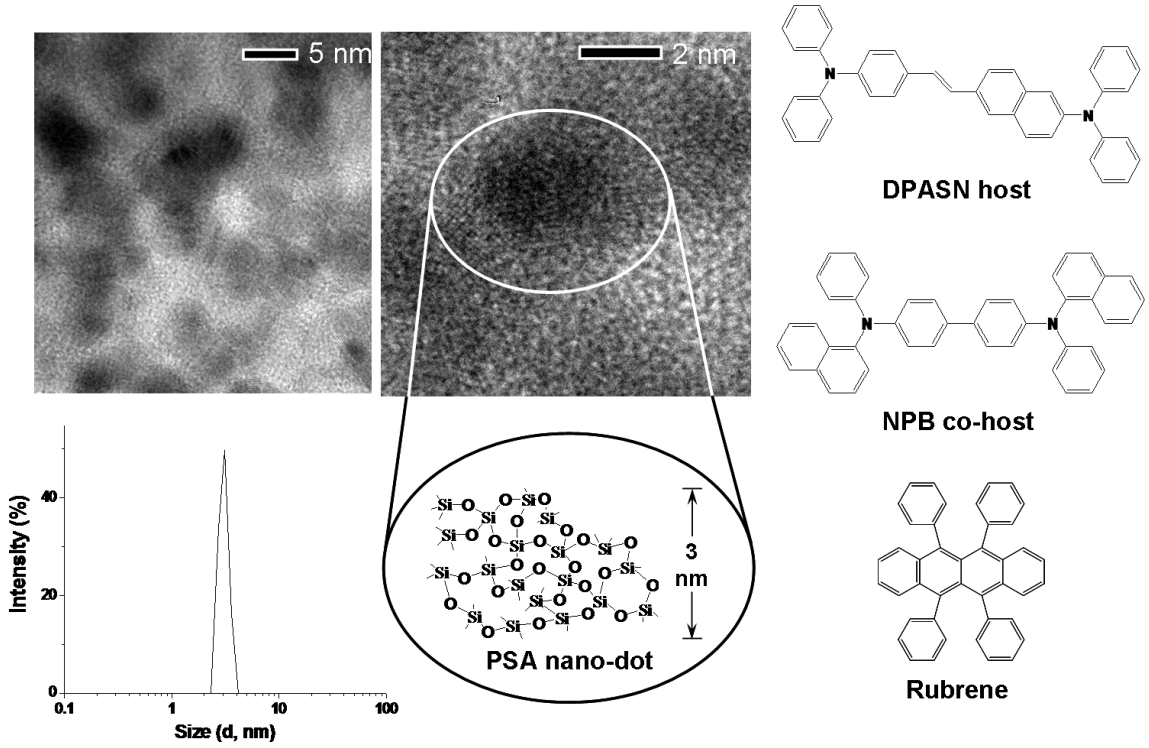

Figure 1. Transmission-electron-microscopic images and dynamic light scattering result of the PSA nanodots studied. Also shown are molecular structures of the PSA nanodot and the two blue light-emitting hosts, DPASN and NPB, and yellow light-emitting guest Rubrene.

molecular structures of the electroluminance (EL) active molecules are also shown in Figure 1. Besides PEDOT:PSS and PEDOT:PSS with incorporated PSA nanodots, another HTL, *N*,*N*,*N*,*N*-tetra(naphthalene-2-yl)phenylenediamine (t-NPD) was studied for comparison. Moreover, the typical device VI of NPB as HTL and Alq_3 as ETL were benefit from the comparison. The best efficiency of the resultant pure-white device with incorporated PSA nanodots was 17.1 lm W^{-1} or 17.6 cd A^{-1} at 100 cd m^{-2}, which is the highest among all reported fluorescent pure-white OLEDs.

It is noteworthy that the efficiency improvement is achieved by adding nanodot into HTL. The devices are composed of host and guest of fluorescent type. The same concept may be applied on phosphorescent OLEDs since the improvement is not on the light emitting layer. Study of the incorporation of PSA nanodot on phosphorescent OLEDs is worthy pursuing.

2. Results and Discussion

The effects of incorporating PSA nanodots and the way in which they are incorporated, by continuous-layer deposition or dispersion, on the EL performance of fluorescent white OLEDs using different HTLs are summarized in Table 1. The power (current) efficiency of the device with t-NPD as the HTL (Device I) was 11.5 lm W^{-1} (13.1 cd A^{-1}) at 100 cd m^{-2} with pure-white emission, the Commission Internationale de l'Eclairage (CIE) coordinates of which were (0.32, 0.36). On adding a thin (9 nm) layer of PSA nanodots in front of the t-NPD HTL (Device II), the power (current) efficiency was decreased to 5.8 lm W^{-1} (11.0 cd A^{-1}) at 100 cd m^{-2}, the emission having CIE coordinates of (0.37, 0.44).

On replacing the HTL of vapor-deposited t-NPD with solution-cast PEDOT:PSS (Device III), the power (current) efficiency was increased from 11.5 lm W^{-1} (13.1 cd A^{-1}) to 13.5 lm W^{-1} (15.4 cd A^{-1}) at 100 cd m^{-2}, the emission having CIE coordinates of (0.31, 0.34). However, spin-coating a thin (9 nm) layer of PSA nanodots in front of the PEDOT:PSS (Device IV) decreased the power (current) efficiency from 13.5 lm W^{-1} (15.4 cd A^{-1}) to 12.3 lm W^{-1} (13.6 cd A^{-1}) at 100 cd m^{-2}, the CIE coordinates of the emission being (0.31, 0.34).

Surprisingly, the device efficiency was significantly improved when PSA nanodots were dispersed into the PEDOT:PSS HTL. For example, the power (current) efficiency of Device V increased markedly from 12.3 lm W^{-1} (13.6 cd A^{-1}) to 17.1 lm W^{-1} (17.6 cd A^{-1}) at 100 cd m^{-2} as the PSA nanodots were predispersed in the PEDOT:PSS HTL by means of pre-mixing in the solution state. (Fig. 2a and b) This marked increase in efficiency may be attributed to a more balanced carrier injection due to the addition of the PSA nanodots to the HTL.

It is noteworthy that in small molecules, the external quantum efficiency (EQE) is believed to be ~ 5 % maximum independent of charge balance.[22,23] However, these nanodots incorporated OLEDs exhibit greater than 5 % EQE. Specifically, the three devices, Devices III to V, all had an EQE greater than 7 %. Amongst, Device V shows a maximum EQE of 8.4 % at current density of 0.101 mA cm^{-2}, as shown in Figure 2b inset. Besides having comparatively low carrier-injec-

Table 1. Effects of PSA nanodot incorporation and incorporating method on the EL characteristics of the fluorescent white OLEDs with different hole-transporting-layers.

Device	HTL	EML		ETL	Driving voltage at 10 cd m^{-2}	Power Efficiency at 100, 1000 cd m^{-2}	Current efficiency at 100, 1000 cd m^{-2}	External quantum efficiency at 100 cd m^{-2}	CIE 1931 coordinates at 100 cd m^{-2}
		NPB	DPASN		[V]	[lm W^{-1}]	[cd A^{-1}]	(%)	
I	t-NPD	100	–	TPBi	3.7	6.1, 4.2	7.8, 8.4	4.3	(0.38, 0.43)
		50	50		3.1	11.5, 7.6	13.1, 12.5	5.6	(0.32, 0.36)
		–	100		3.0	9.5, 6.2	10.1, 11.1	5.2	(0.30, 0.35)
II	PSA/t-NPD	50	50	TPBi	4.4	5.8, 3.2	11.0, 9.3	4.9	(0.37, 0.44)
III	PEDOT	50	50	TPBi	3.1	13.5, 8.3	15.4, 12.7	7.2	(0.31, 0.34)
IV	PSA/PEDOT	50	50	TPBi	3.2	12.3, 7.5	14.6, 12.7	7.0	(0.31, 0.34)
V	PEDOT with PSA	50	50	TPBi	3.1	17.1, 12.2	17.6, 15.9	8.3	(0.30, 0.34)
VI	NPB	50	50	Alq3	3.0	3.1, 1.8	4.3, 4.5	2.4	(0.38, 0.50)

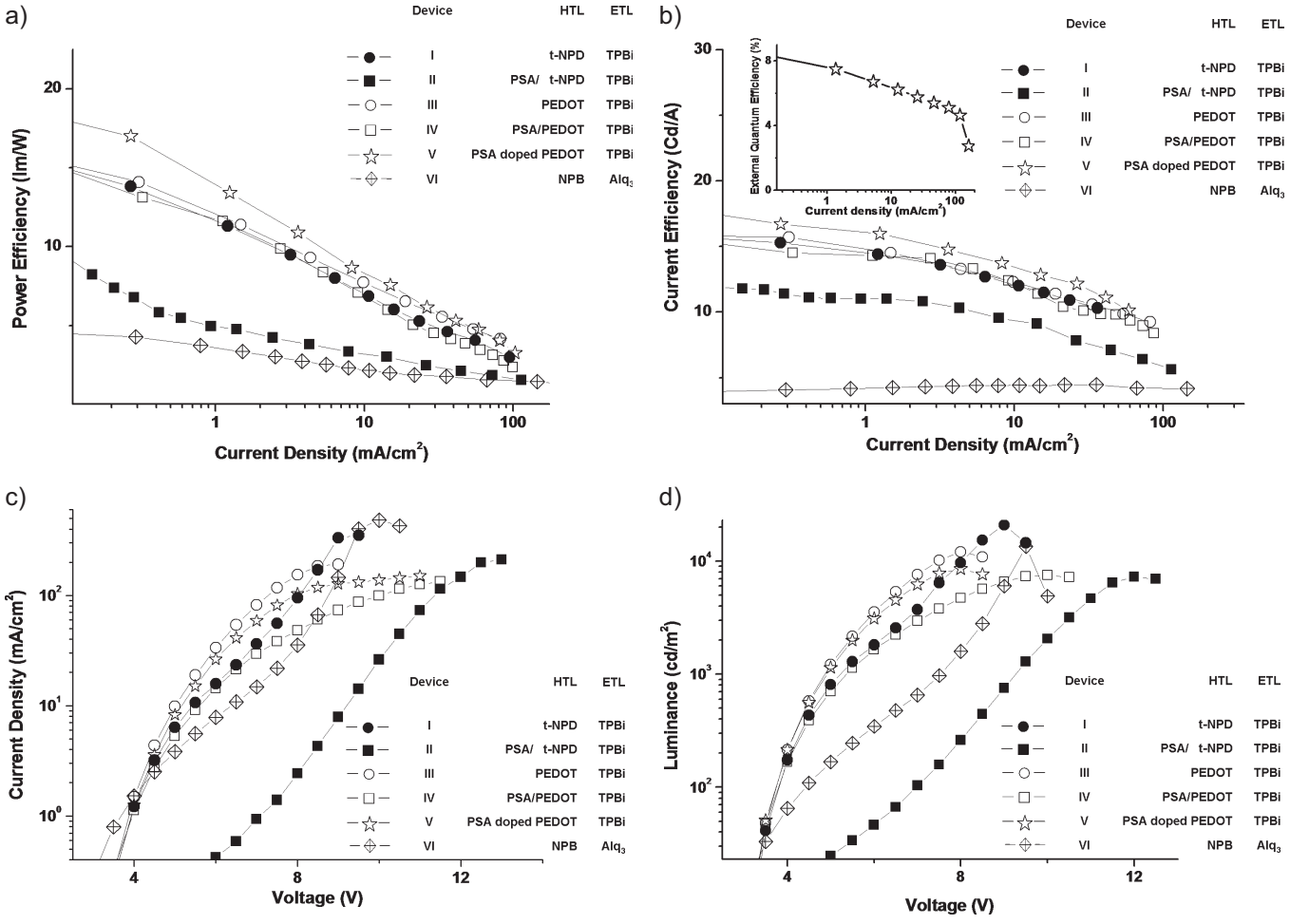

Figure 2. a) Effects of PSA nanodot incorporation and incorporating method on the resultant power efficiency of the fluorescent white OLEDs with mixed-host structure using different hole-transporting-layers. b) Effects of PSA nanodot incorporation and incorporating method on the resultant current efficiency of the fluorescent white OLEDs with mixed-host structure using different hole-transporting-layers. The inset shows the external quantum efficiency of Device V. c) Effects of PSA nanodot incorporation and incorporating method on the resultant current density of the fluorescent white OLEDs with mixed-host structure using different hole-transporting-layers. d) Effects of PSA nanodot incorporation and incorporating method on the resultant luminance of the fluorescent white OLEDs with mixed-host structure using different hole-transporting-layers.

tion barriers, these devices should plausibly have a more balanced injection of holes against that of electrons. Since excessive holes injected into the EML frequently result in a less balanced carrier-injection and consequently a poorer EL-efficiency, trapping excessive holes in the HTL would be effective in efficiency improvement. When the HTL of t-NPD was re-

placed by that of PEDOT, better carrier-injection balance may have been obtained for the resultant device (Device III) as indicated by its comparatively lower current density, which was 0.325 mA cm^{-2} at 3.5 V, while 0.341 mA cm^{-2} for Device I. By incorporating the PSA nanodot into the HTL of PEDOT (Device V), much better carrier-injection balance must have been obtained by realizing its current density was further reduced to 0.269 mA cm^{-2}.

Furthermore, the incorporation of PSA nanodot into the HTL can effectively trap holes, preventing excessive holes consuming, which may lead to exciton-quenching phenomena.[24] The concentrations of holes may thus be more equivalent to that of electrons, increasing holes-electrons recombination probability and electrons-photons conversion efficiency (internal quantum efficiency), and higher EQE would hence be obtained.

Typically, excessive hole injection is one root cause of a less efficient device with unbalanced carrier injection.[25–27] A proper reduction of the hole injection would sometimes help to improve the device efficiency. The synthesized PSA nanodots described here exhibited a negative charge on the surface, which would preferably trap the holes entering the HTL from the ITO cathode. This trapping mechanism would consequently reduce the injection of holes into the emissive layer, leading to a more balanced injection of holes and electrons. The reduction of hole injection can be revealed by a decrease in the current density of the studied device. The incorporation of PSA nanodots into the PEDOT:PSS HTL via pre-mixing (Device V) had indeed markedly reduced the current density, as shown in Figure 2c. Since its corresponding luminance was barely affected, this explains why Device V was significantly more efficient. The incorporation of PSA nanodot that could effectively decrease the hole injection can be revealed from the *J–V* curves of Devices III, IV, and V shown in Figure 2c. The current density, at 3.5 V, for example, decreases from 0.325 to 0.306 mA cm^{-2} as a 70 Å PSA nanodot layer is added between ITO and PEDOT. The current density also decreases to 0.269 mA cm^{-2} as 7.0 wt % PSA nanodot is incorporated into the PEDOT layer. Although the reduction of current density was more marked for Device IV, its efficiency did not improve because the corresponding luminance was greatly reduced, probably due to the formation of a hole-injection barrier layer of PSA in between the ITO and PEDOT layers (Fig. 2d).

The comparatively low current density of Device II may also be attributed to the formation of a continuous barrier layer of PSA nanodots (Fig. 3). The poor carrier-transporting characteristics of the film of PSA nanodots could also be revealed by the comparatively high driving voltage of Device II, which was 4.4 V to trigger 10 cd m^{-2}. The driving voltages of the other devices were 3.2 V or less. The carrier-transporting property may have been improved, more or less, for Device IV as the HTL was changed from t-NPD to PEDOT and the corresponding deposition method was changed from the dry- to wet-process. The poor carrier-transporting properties of Device IV may perhaps have arisen as the HTL was changed from t-NPD to PEDOT and the corresponding deposition method was changed from a dry to a wet process. It is very likely that during the dispersion and spin-coating processes, the solvent in the

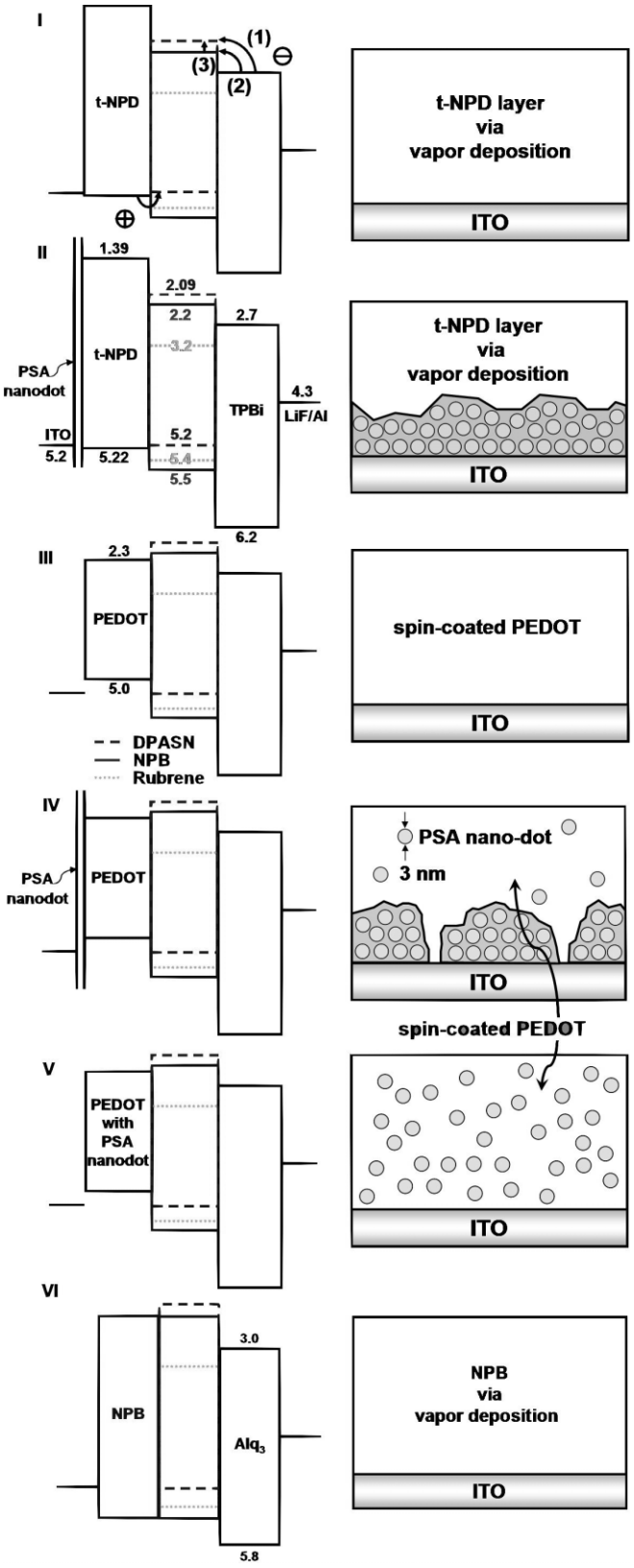

Figure 3. HOMO/LUMO energy-level diagrams of the fluorescent white OLEDs with five different HTLs with and without PSA nanodot incorporation. Schematic illustrations show the plausible effects of PSA nanodot incorporation method and deposition process, wet or dry, of the HTL on the distribution of the added PSA nanodots on top of indium tin oxide.

ADVANCED FUNCTIONAL MATERIALS

PEDOT-containing solution may have penetrated into the previously formed PSA nanodot layer and created space for the PEDOT to come directly into contact with the ITO cathode.

By pre-mixing the PSA nanodots into the PEDOT solution before spin coating (Device V), they become well dispersed throughout the PEDOT layer and do not form a continuous barrier layer to hole-injection. On the other hand, the resultant PEDOT can be in good direct contact with the ITO layer, minimizing any unfavorable effects on the injection of holes from the ITO to the HTL, while keeping the hole-trapping function of the PSA nanodots effective within the HTL. This explains why Device V exhibited the highest efficiency. However, the addition of the PSA nanodots should have reduced the injection of holes into the HTL so that the resultant brightness always decreased as the PSA nanodots were added, regardless of the HTL employed or the way the nanodots were applied.

Compared with Device V (3.1 V), Device VI has a lower driving voltage of 3.0 V. However, the lower driving voltage does not result in a higher power efficiency. Contrarily, its efficiency is 3.1 lm W^{-1}, much lower than that of Device V (17.1 lm W^{-1}). The low efficiency of Device VI may be attributed to the shift of the recombination zone from the desired EML to the low EL-efficiency greenish Alq_3. The shift can be evidenced by the resultant emissive color change from pure white (0.30, 0.34) in Device V to yellow-greenish (0.38, 0.50) in Device VI.

The doping of PSA nanodot has slightly increased the surface roughness of the PEDOT film; i.e., its surface roughness is increased from 1.6 to 1.7 nm as PSA nanodot is incorporated, as shown in Figure 4a and b. However, with or without PSA nanodot, the coating of PEDOT has significantly smoothed out the surface of ITO, whose surface roughness is 2.7 nm before the PEDOT is coated, as shown in Figure 4c. It may be concluded that the minor morphological variation is not the main cause of the marked efficiency improvement.

The lifetime of the device was increased from (42 ± 0.8) to (61 ± 1.5) hours as 7.0 wt % of PSA nanodot was doped into the HTL, as shown in Figure 5. The lifetime improvement may be attributed to the facts that lesser holes were injected into the EML so that charge-accumulation-caused damage may be reduced, and the resultant higher device efficiency could somewhat reduce heat generated upon emission, preventing damage caused by the generation of excessive heat during operation.[28,29]

The high efficiency of Device V may also be attributed to the use of the mixed host of NPB and DPASN. For example, the power (current) efficiency of the device with a pure NPB host was 6.1 lm W^{-1} (7.8 cd A^{-1}) at 100 cd m^{-2}, while it was 9.5 lm W^{-1} (10.1 cd A^{-1}) when using a pure DPASN host. By blending NPB with DPASN as a mixed host, the resultant device showed a synergistic increase in efficiency. The highest efficiency, 11.5 lm W^{-1} (13.1 cd A^{-1}) at 100 cd m^{-2}, was observed when 50 wt % NPB was mixed with 50 wt % DPASN. This was much greater than the efficiency of either pure-host counterpart.

This synergistic increase in efficiency may be attributed to the new cascading routes with lower electron-injection barriers that were generated when the mixed host was employed. As shown in the energy diagram of Device I in Figure 3, the injection of electrons from the TPBi electron-transporting layer (ETL) to the emission layer (DPASN), via route (1), is the bottleneck to forming balanced carrier-injection. This is because its injection barrier is 0.61 eV, much greater than that for the injection of holes from the HTL (t-NPD), which is –0.02 eV. Upon the addition of NPB, a new path for electrons to enter

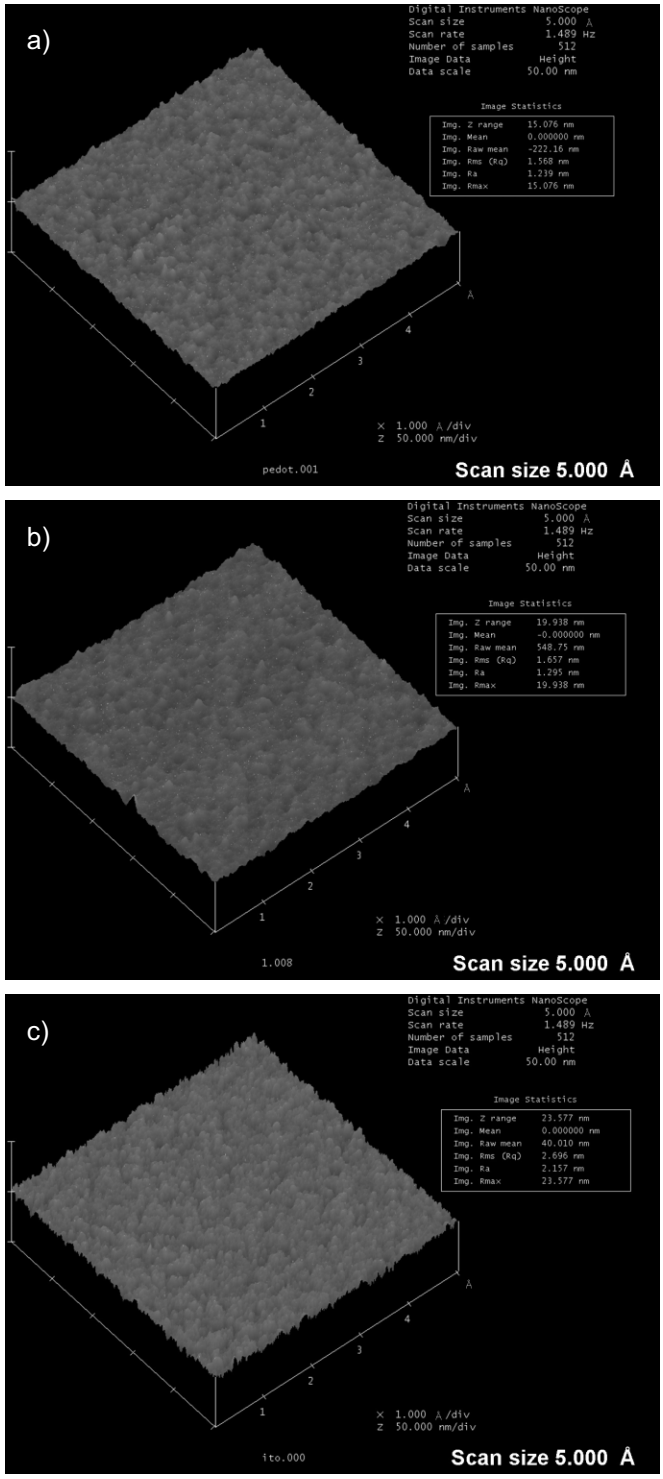

Figure 4. a) AFM image of PEDOT spin-coated ITO substrate. b) AFM image of PEDOT with PSA nanodot spin-coated ITO substrate. c) AFM image of ITO surface.

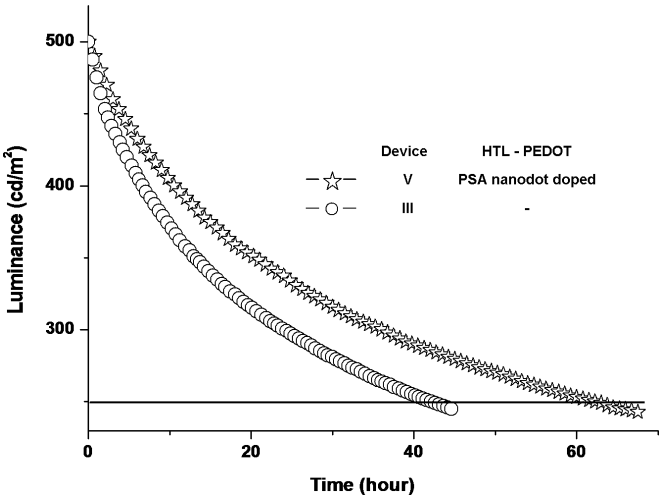

Figure 5. Effects of PSA nanodot incorporation on the lifetime of white OLEDs driven under constant current with an initial brightness of 500 cd m^{-2} at room temperature.

the DPASN host from the ETL was formed, namely, first route (2) and then route (3), with electron-injection barriers of 0.5 and 0.11 eV, respectively. Regardless of whether a pure DPASN host or a mixed host of DPASN with NPB was used, the holes from the HTL preferred to enter the DPASN host since it did not exhibit an injection barrier to hole, while the injection barrier for holes to enter the NPB co-host was 0.28 eV. As a result, most of the entering holes would accumulate on the DPASN host. Originally, electrons preferably entered directly into the NPB host instead of the DPASN host because the electron-injection barrier of the NPB host was comparatively lower than that of the DPASN counterpart. Since only very few of the electrons in the NPB host would be consumed to form excitons due to the lack of entering holes, the excess electrons in the NPB host would eventually be forced to jump into the DPASN host. This process would favour the generation of more excitons there, consequently resulting in brighter blue emission from the DPASN host and, via energy transfer, brighter yellow emission from Rubrene, leading to the observed emission of bright white light with a relatively high efficiency.

3. Conclusion

The best reported efficiency of 17.1 lm W^{-1} (or 17.6 cd A^{-1}) with 100 cd m^{-2} at 3.1 V for a fluorescent pure-white OLED was obtained by incorporating small PSA nanodots into the hole-transporting layer of a device with a mixed-host structure. The marked improvement in efficiency may be attributed to both a more balanced injection of holes and electrons upon the addition of the PSA nanodots and the introduction of cascading routes with lower electron-injection barriers upon the addition of a new host of NPB to the original DPASN host. These cascading routes favored the injection of electrons into the DPASN and also the generation of more excitons there.

4. Experimental

The WOLEDs of luminance and CIE chromatic coordinates results were measured by using Minolta CS-100 luminance-meter. The lifetimes were obtained using a Minolta CS-1000S spectrophotometer. The highest occupied molecular orbital (HOMO) energy levels of the organic materials studied were calculated from their oxidation potentials measured by a cyclicvoltammetry,[30] while the corresponding lowest unoccupied molecular orbital energy levels were estimated based on their HOMO energy levels and the lowest-energy absorption edge of the UV-visible adsorption spectra. A Keithley 2400 electrometer was used to measure the current–voltage (*I–V*) characteristics. The atomic force microscopy (AFM) images of conductive film were characterized by Nanoscope DI3100. The EQE was then calculated directly from the EL characteristics and spectra of the devices.[31]

Received: April 17, 2007
Revised: September 5, 2007
Published online: December 18, 2007

[1] A. R. Duggal, J. J. Shiang, C. M. Heller, D. F. Foust, *Appl. Phys. Lett.* **2002**, *80*, 3470.
[2] B. W. D'Andrade, S. R. Forrest, *Adv. Mater.* **2004**, *16*, 1585.
[3] J. Kido, M. Kimura, K. Nagai, *Science* **1995**, *267*, 1332.
[4] Z. Shen, P. E. Burrows, V. Bulovic, S. R. Forrest, M. E. Thompson, *Science* **1997**, *276*, 2009.
[5] C. W. Tang, S. A. Vanslyke, C. H. Chen, *J. Appl. Phys.* **1989**, *65*, 3610.
[6] B. W. D'Andrade, R. J. Holmes, S. R. Forrest, *Adv. Mater.* **2004**, *16*, 624.
[7] Y. Shao, Y. Yang, *Appl. Phys. Lett.* **2005**, *86*, 073510.
[8] Y. S. Huang, J. H. Jou, W. K. Weng, J. M. Liu, *Appl. Phys. Lett.* **2002**, *80*, 2782.
[9] R. F. Service, *Science* **2005**, *310*, 1762.
[10] J. H. Jou, Y. S. Chiu, C. P. Wang, R. Y. Wang, H. C. Hu, *Appl. Phys. Lett.* **2006**, *88*, 193501.
[11] J. H. Jou, Y. S. Chiu, R. Y. Wang, H. C. Hu, C. P. Wang, H. W. Lin, *Org. Electron.* **2006**, *7*, 8.
[12] M. Ikai, S. Tokito, Y. Sakamoto, T. Suzuki, Y. Taga, *Appl. Phys. Lett.* **2001**, *79*, 156.
[13] H. Kanno, Y. Sun, S. R. Forrest, *Appl. Phys. Lett.* **2006**, *89*, 143516.
[14] C. H. Chuen, Y. T. Tao, *Appl. Phys. Lett.* **2002**, *81*, 4499.
[15] G. Li, J. Shinar, *Appl. Phys. Lett.* **2003**, *83*, 5359.
[16] Y. Sun, N. C. Giebink, H. Kanno, B. Ma, M. E. Thompson, S. R. Forrest, *Nature* **2006**, *440*, 908.
[17] J. H. Jou, P. H. Chiang, Y. P. Lin, C. Y. Chang, C. L. Lai, *Appl. Phys. Lett.* **2007**, *91*, 043504.
[18] S. A. Carter, J. C. Scott, P. J. Brock, *Appl. Phys. Lett.* **1997**, *71*, 1145.
[19] G. Gustafsson, Y. Cao, G. M. Treacy, F. Klavetter, N. Colaneri, A. J. Heeger, *Nature* **1992**, *357*, 477.
[20] J. H. Jou, M. C. Sun, H. H. Chou, C. H. Li, *Appl. Phys. Lett.* **2005**, *87*, 043508.
[21] Y. G. Hsu, C. P. Wang, *J. Polym. Res.* **2003**, *10*, 201.
[22] J. Kido, Y. Iizumi, *Appl. Phys. Lett.* **1998**, *73*, 2721.
[23] M. Pope, C. E. Swenberg, in *Electronic Processes in Organic Crystals*, Oxford University Press, New York, NY **1982**, p. 64.
[24] L. Yan, N. J. Watkins, S. Zorba, Y. Gao, C. W. Tang, *Appl. Phys. Lett.* **2002**, *81*, 2752.
[25] C. O. Poon, F. L. Wong, S. W. Tong, R. Q. Zhang, C. S. Lee, S. T. Lee, *Appl. Phys. Lett.* **2003**, *83*, 1038.
[26] F. Zhu, B. Low, K. Zhang, S. Chua, *Appl. Phys. Lett.* **2001**, *79*, 1205.
[27] Z. B. Deng, X. M. Ding, S. T. Lee, W. A. Gambling, *Appl. Phys. Lett.* **1999**, *74*, 2227.
[28] Y. C. Tsai, J. H. Jou, *Appl. Phys. Lett.* **2006**, *89*, 243521.
[29] H. Aziz, Z. D. Popvic, *Chem. Mater.* **2004**, *16*, 4522.
[30] S. Janietz, D. D. C. Bradley, M. Grell, C. Giebler, M. Inbasekaran, E. P. Woo, *Appl. Phys. Lett.* **1998**, *73*, 2453.
[31] S. R. Forrest, D. D. C. Bradley, M. E. Thompson, *Adv. Mater.* **2003**, *15*, 1043.